The Effect of Space-charge and Wake Fields in the Fermilab Booster*

Alexandru Macridin, Panagiotis Spentzouris, James Amundson, Fermilab, Batavia, Illinois 60510, USA
Linda Spentzouris, Daniel McCarron, Illinois Institute of Technology, Chicago, Illinois, USA

Abstract

We calculate the impedance and the wake functions for laminated structures with parallel-planes and circular geometries. We critically examine the approximations used in the literature for the coupling impedance in laminated chambers and find that most of them are not justified because the wall surface impedance is large. A comparison between the flat and the circular geometry impedance is presented. We use the wake fields calculated for the Fermilab Booster laminated magnets in realistic beam simulations using the Synergia code. We find good agreement between our calculation of the coherent tune shift at injection energy and the experimental measurements.

INTRODUCTION

Wake fields have a strong effect on the high intensity beam dynamics in accelerators, being a major cause for losses and instabilities. While there is a satisfactory knowledge of the wake fields in metallic chambers with smooth geometries, the attempts to describe the impedance effect in structures with laminations are not in very good agreement with the measured data.

Aside from a better calculation of the impedance, realistic simulations which consider the interplay between the wake fields and other effects in accelerators should be employed to describe beam dynamics and for comparison with measurements. We use the Synergia code [1] developed at Fermilab to run beam dynamics simulations. Synergia is designed to simulate complex beam dynamics, employing high order maps to describe single particle propagation through accelerators and considers collective effects such as space charge (SC) forces and wake field interactions.

The Fermilab Booster is a good example of a machine where the beam is exposed to laminations, showing large impedance effects [2, 3]. There are several calculations of the impedance in laminated structures with applications for the Fermilab Booster [4, 5, 6, 7]. Most of them [4, 5, 6] address only the circular geometry which can be argued not to be very appropriate for the Booster magnets. Ng [7] addresses both the parallel-plane geometry, which is close to the real geometry of the Booster magnets [8], and the transverse impedance. However he assumes a beam which extends to infinity on the horizontal direction. While this approximation works for metallic pipes, we find it to produce wakes too large for the laminated chambers.

In this paper we calculate the impedance and the wake functions for laminated structures with parallel-planes and circular geometries. The commonly used approximations for resistive-wall impedance of metallic chambers are not valid here because the surface impedance is large. A comparison between the circular and the parallel-planes chamber results is shown. The wake functions are used in Synergia simulations of the Booster machine. The transverse tune shift calculated from simulations is in good agreement with the experiment [3].

COUPLING IMPEDANCE

Parallel-planes chambers

Consider a vacuum chamber made by two parallel planes separated by a distance $2b$ along y-direction and a beam propagation along z-direction. We look for synchronous solutions of Maxwell's equations,

$$\vec{E},\vec{H}(x,y,z,t) \quad = \quad \vec{E},\vec{H}(\eta,y)e^{-j(\eta x+kz-\omega t)} \quad (1)$$

in the relativistic limit $k=\frac{\omega}{c}$.

The boundary conditions at the chamber wall determine the surface impedances defined as $\mathcal{R}_z(\eta)=\frac{E_z(\eta,b)}{H_x(\eta,b)}$ and $\mathcal{R}_x(\eta)=-\frac{E_x(\eta,b)}{H_z(\eta,b)}$. The coupling impedance can be written as function of wall surface impedances as

$$Z^{||}=\int_0^\infty \frac{\operatorname{sech}^2\eta b\,\mathcal{R}_z(\eta)/(2\pi)d\eta}{1+j\frac{\mathcal{R}_z(\eta)}{Z_0}(\frac{k}{\eta}-\frac{\eta}{k})\operatorname{th}\eta b+\frac{\mathcal{R}_z(\eta)\mathcal{R}_x(\eta)}{Z_0^2}\operatorname{th}^2\eta b} \quad (2)$$

$$Z_y=\int_0^\infty \frac{\eta^2\operatorname{csch}^2\eta b\,\mathcal{R}_z(\eta)/(2\pi k)d\eta}{1+j\frac{\mathcal{R}_z(\eta)}{Z_0}(\frac{k}{\eta}-\frac{\eta}{k})\operatorname{cth}\eta b+\frac{\mathcal{R}_z(\eta)\mathcal{R}_x(\eta)}{Z_0^2}\operatorname{cth}^2\eta b} \quad (3)$$

$$Z_x=\int_0^\infty \frac{\eta^2\operatorname{sech}^2\eta b\,\mathcal{R}_z(\eta)(2\pi k)d\eta}{1+j\frac{\mathcal{R}_z(\eta)}{Z_0}(\frac{k}{\eta}-\frac{\eta}{k})\operatorname{th}\eta b+\frac{\mathcal{R}_z(\eta)\mathcal{R}_x(\eta)}{Z_0^2}\operatorname{th}^2\eta b} \quad (4)$$

For metallic chambers with large conductivity σ, ($Z_0\sigma\approx 10^8-10^9 m^{-1}$)

$$\mathcal{R}_z(\eta),\mathcal{R}_x(\eta)\approx\frac{1+j}{\delta\sigma}\,, \quad (5)$$

where δ is the skin penetration depth. In this case $\mathcal{R}_z$, $\mathcal{R}_x$ are small, of order O($\frac{1}{\sqrt{Z_0\sigma}}$) and independent of η. Therefore the commonly used approximation for metallic pipe

* This work was supported by the United States Department of Energy under contract DE-AC02-07CH11359 and the ComPASS project funded through the Scientific Discovery through Advanced Computing program in the DOE Office of High Energy Physics. This research used resources of the National Energy Research Scientific Computing Center, which is supported by the Office of Science of the U.S. Department of Energy under Contract No. DE-AC02-05CH11231 and of the Argonne Leadership Computing Facility at Argonne National Laboratory, which is supported by the Office of Science of the U.S. Department of Energy under contract DE-AC02-06CH11357.

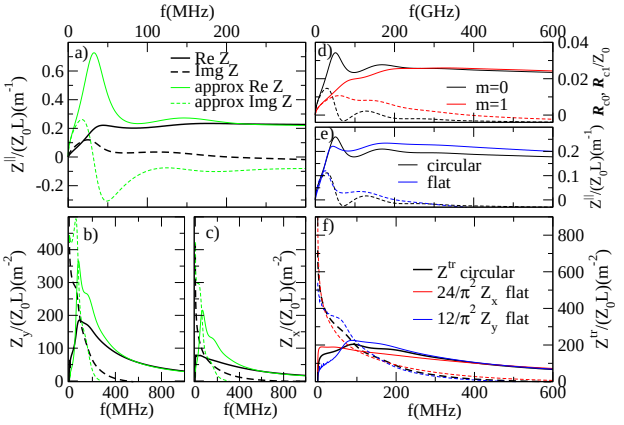

Figure 1: Laminated chamber with $b = 2.1cm$, $d = 15.24cm$, $h = 9.52 \times 10^{-4}cm$, $\tau = 6.35 \times 10^{-2}cm$, $\epsilon_{1r} = 4.75$, $\mu_{2r} = 100$, and $\sigma_2 = 0.5 \times 10^7 (\Omega m)^{-1}$ (iron), specific to the Fermilab Booster F-magnet. a), b) & c) Longitudinal, horizontal and vertical coupling impedance for parallel-planes chamber. The green lines are calculated by neglecting the η dependence of the surface impedance. d) Crack surface impedance for $m = 0$ (black) and $m = 1$ (red) for circular chamber. e) & f) Longitudinal and transverse impedance for circular chamber (black). The parallel-planes impedance also shown with blue and red. For comparison the horizontal impedance is multiplied by $\frac{24}{\pi^2}$ (red) and the vertical one by $\frac{12}{\pi^2}$ (blue).

impedance is

$$Z^{||} = \frac{\mathcal{R}_z}{2\pi b},\ Z_x = \frac{\mathcal{R}_z}{2\pi k}\frac{\pi^2}{12b^3},\ Z_y = \frac{\mathcal{R}_z}{2\pi k}\frac{\pi^2}{6b^3}\ . \tag{6}$$

However when the surface impedance is large or η dependent, as it is for laminated structures, these approximations are not valid and Eqs. 2, 3 and 4 should be used instead.

In structures with laminations the longitudinal surface impedance can be written as

$$\mathcal{R}_z = \frac{\mathcal{R}_{1z}h + \mathcal{R}_{2z}\tau}{h+\tau}\ , \tag{7}$$

where the subscripts "1" denotes the dielectric crack of width h and "2" denotes the metallic lamination of width τ. We assume that the laminations are shorted by an ideal conductor at distance d from the chamber's center. The lamination longitudinal surface impedance as well the chamber horizontal surface impedance can be approximated by the usual metal-vacuum boundary surface impedance $\mathcal{R}_{2z}, \mathcal{R}_x \approx \frac{1+j}{\delta_2\sigma_2}$. By solving the Maxwell's equations inside the crack and inside the lamination regions one gets for the crack surface impedance

$$\frac{\mathcal{R}_{1z}(\eta,\omega)}{Z_0} = j\frac{q^2+\eta^2}{q\frac{\omega}{c}\epsilon_{1r}}\tan q(d-b) \tag{8}$$

where

$$q^2 = \omega^2\epsilon_1\mu_1[1+(1-j)\frac{\mu_2}{\mu_1}\frac{\delta_2}{h}] - \eta^2\ . \tag{9}$$

Note that $\mathcal{R}_{1z}$ in η dependent. Neglecting this and considering $\mathcal{R}_{1z}(\eta) = \mathcal{R}_{1z}(0)$, as it has been done in Ref [7], would yield significantly larger impedance functions.

The impedance for a chamber with parameters specific to the Booster F magnet is illustrated in Figs. 1a, 1b and 1c. Note that the approximation which neglects the η depenedence of $\mathcal{R}_{1z}$ yields larger impedance below frequencies $\sim 500MHz$.

Circular chambers

In a round chamber of radius b the coupling impedance can be written as

$$Z_0^{||} = \frac{\frac{\mathcal{R}_{z0}}{2\pi b}}{1+j\frac{\mathcal{R}_{z0}}{Z_0}\frac{kb}{2}} \tag{10}$$

for the angular number $m = 0$, and

$$Z_m^{\perp} = \frac{c}{\omega}Z_m^{||} = \frac{\frac{c\mathcal{R}_{zm}}{\omega\pi b^{2m+1}}}{1+j\frac{\mathcal{R}_{zm}}{Z_0}(\frac{kb}{m+1}-\frac{m}{bk})+\frac{\mathcal{R}_{zm}\mathcal{R}_{\theta m}}{Z_0^2}}, \tag{11}$$

for $m \geq 1$, where $\mathcal{R}_{zm} = \frac{E_{zm}}{H_{\theta m}}|_{r=b}$, $\mathcal{R}_{\theta m} = -\frac{E_{\theta m}}{H_{zm}}|_{r=b}$.

For metallic chambers the surface impedances are given by Eq. 5 for all m. Since they are small the following approximations are common

$$Z^{||} = \frac{\mathcal{R}_z}{2\pi b},\ Z_1^{\perp} = \frac{\mathcal{R}_z}{\pi k b^3},\ Z_1^{\perp} = \frac{2c}{\omega b^2}Z_0^{||}\ . \tag{12}$$

These approximations are not valid in laminated chambers.

When laminations are present, Eq. 7 determines the longitudinal surface impedance. From Maxwell's equations solution in the crack and in the lamination regions one gets

$$\frac{\mathcal{R}_{1zm}}{Z_0} = -j\frac{qc}{\omega\epsilon_{r1}}\frac{J_m(qb)Y_m(qd)-Y_m(qb)J_m(qd)}{J'_m(qb)Y_m(qd)-Y'_m(qb)J_m(qd)} \tag{13}$$

where

$$q^2 = \omega^2\epsilon_1\mu_1[1+(1-j)\frac{\mu_2}{\mu_1}\frac{\delta}{h}]\ . \tag{14}$$

The lamination and the angular surface impedance are $\mathcal{R}_{2z}, \mathcal{R}_{\theta m}(m \geq 1) \approx \frac{1+j}{\delta_2\sigma_2}$. Note that, unlike the round metallic chamber case, the surface impedance $\mathcal{R}_{zm}$ is m dependent. The difference between the $m = 0$ and the $m = 1$ crack surface impedance can be seen in Fig. 1d. Since, up to the first order in beam displacement, the longitudinal and transverse wakes correspond to $m = 0$ and $m = 1$ respectively there is no such simple relation between $Z_0^{||}$ and $Z_1^{\perp}$ as in Eq. 12.

The longitudinal and the transverse coupling impedance for laminated circular chambers are shown in Figs.1e and respectively 1f. For comparison the parallel-planes impedances are also shown. To account for the geometry difference the vertical impedance was multiplied by $\frac{12}{\pi^2}$ while the horizontal one by $\frac{24}{\pi^2}$. Note that the circular and the flat impedances are different below $500MHz$ for parameters specific to the Booster magnets.

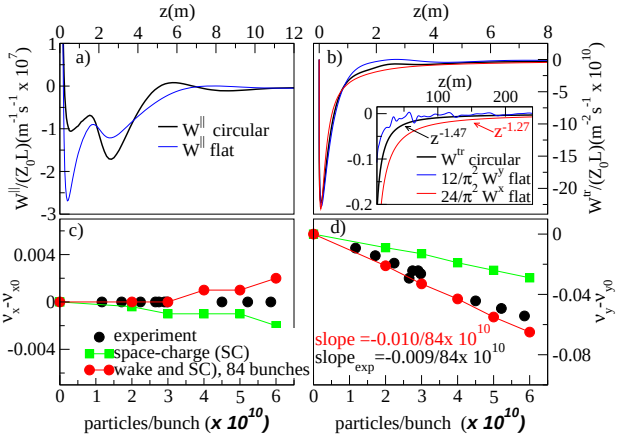

Figure 2: a) & b) Same parameters as in Fig. 1. Longitudinal and transverse wakes for circular chamber (black). The parallel-planes wake shown with blue and red. The horizontal wake is multiplied by $\frac{24}{\pi^2}$ (red) and the vertical one by $\frac{12}{\pi^2}$ (blue). Inset: The long distance behavior of transverse wakes. The transverse wake for round chamber decays as $z^{-1.47}$ while the parallel-planes horizontal wake decays as $z^{-1.27}$. c) & d) Coherent horizontal and respectively vertical tune shift versus beam intensity. The estimated tune uncertainty in calculations is less than 0.001. The vertical tune is suppressed while the horizontal tune changes very little. Space charge (SC) suppresses both the vertical and the horizontal tunes, while the coupling wake suppresses the vertical tune and increases the horizontal tune. The calculation are in good agreement with the experiment, the deviation being within a 3 σ_{meas} range.

The wake functions for the circular and the flat chambers are shown in Fig.2a and Fig.2b. The flat longitudinal wake has a larger attractive peak at $|z| \approx 0.5m$ while the circular wake is stronger at $|z| \approx 3m$. The transverse circular wake decays faster with distance at large z than the horizontal parallel-planes wake. Since the latter is important for the quadrupole tune shift in flat chambers [9], using circular wakes weighted by the geometric factors $\frac{\pi^2}{24}$ and $\frac{\pi^2}{12}$ to describe this effect would underestimate the tune shift.

COHERENT TUNE SHIFT

We employ the Synergia code to run realistic beam simulations for the Fermilab Booster. In order to model the Booster we developed new 3D SC solvers suitable for parallel-planes and rectangular vacuum chambers for Synergia. We also developed new modules to simulate the laminated wake fields described in the previous section. The Booster has 24 cells, each cell including F-magnets and D-magnets and circular pipe drift sections [3, 8]. For each of these constituent elements we consider suitable wake field and SC solvers.

The simulation is initialized with a six-dimensional Gaussian beam matched for propagation without collective effects. The input parameters are $x_{rms} = 0.0086\ m$, $y_{rms} = 0.0032\ m$ and $z_{rms} = 0.88\ m$. We run 84-bunch (full machine) simulations with different beam intensities of up to 6×10^{10} particles per bunch at the injection energy ($400MeV$). These values are similar to those in the Booster during the experimental runs [8]. The phasing of the rf cavities is set up so that there is no net acceleration of the beam. To determine the coherent tunes, we measure the position of the beam center at different locations over 1000 turns. The tunes are extracted from the Fourier transform of the beam center displacement as a function of position.

In Figs. 2c and 2d, simulation of the coherent betatron tune shifts in the horizontal and vertical planes are compared with the experimental data [3] (black circles). Notice that the scale for the vertical tune shift is about 20 times larger than for the horizontal one. The red circles are the results of the simulations which include both space charge and coupling wake fields. The agreement with the experimental data is good, being within 3 σ_{meas} range, where σ_{meas} is the measurement standard deviation. The vertical tunes are decreasing while the horizontal tunes do not change significantly with beam intensity. The green squares show the results when only the space charge interaction (including here the space-charge impedance) is taken into account. For the vertical case, both the wake and the space charge force decrease the tune, the coupling wake having a larger effect. For the horizontal case, the space charge force slightly suppresses the tune, while the wake slightly increases it.

CONCLUSIONS

In this paper we calculate the impedance and the wake functions for laminated structures with parallel-planes and circular geometries. First the coupling impedance is derived as a function of the wall surface impedance. Then the surface impedance is calculated by solving Maxwell's equations inside the lamination and the crack regions. We find that the commonly used resistive-wall approximations, good for metallic pipes with small surface impedance, are not valid in the laminated structures where the surface impedance is large. Realistic Synergia simulations of the Booster machine with wake fields predict transverse coherent tune shifts in good agreement with the experiment [3].

REFERENCES

[1] J. Amundson, *et al*, J. Comp. Phys. 211, 229 (2006).

[2] J. L. Crisp, *et al*, Fermilab Report ,TM-2145, (2001).

[3] Daniel McCarron, Ph. D. Thesis, Fermilab, 2010.

[4] S. C. Snowdon, Fermilab Report TM-277 (1970).

[5] A. G. Rugeira, Fermilab Report , FN-220, (1971).

[6] R. Gluckstern, Fermilab Report , TM-1374, (1985).

[7] K. Y. Ng, Fermilab FN-0744, (2004).

[8] Booster Rookie Book, Fermilab, (2009).

[9] A. Chao, *et al*, Phys. Rev. STAB, 111001 (2002).